

Y. Oura, N. Shirai, S. Shibata¹ and S. Sekimoto¹

Graduate School of Science and Engineering,
Tokyo Metropolitan University

¹Research Reactor Institute, Kyoto University

INTRODUCTION: An instrumental activation analysis method is one of a nondestructive and highest sensitive method. Among activation analysis, instrumental neutron activation analysis (INAA) using (n, γ) reaction are mainly used because it is easy to use reactor neutrons.

Photon activation analysis (PAA) method using (γ , n) reaction by bremsstrahlung from an electron accelerator is a complementary method to INAA and PAA can determine some elements which INAA can not determine. At the present, however, PAA is not used well like NAA. Main reason of a little use is probably that a machine time of an electron accelerator is not sufficient for PAA because an electron accelerator is used by many users in a variety of fields. Furthermore, the other reason is guessed that it is not easy to refer reaction yield values of (γ , n) reactions for calculation of induced radioactivity as cross section values of (n, γ) reactions. In many textbooks on photonuclear reaction, a figure of systemic relation between reaction yield in mole⁻¹R⁻¹ and target atomic number by Kato et al. are inserted. But values in mole⁻¹R⁻¹ are practically not easy to calculate induced activity, therefore values in barn/eq.q. are desired.

In this study a final goal is that absolute reaction yield values in barn/eq.q. of (γ , n) reactions are determined for usefulness to PAA. Since measurement of absolute flux of bremsstrahlung is difficult now, relative reaction yields are determined in the immediate future.

EXPERIMENTS: Target nuclides in this year were ²³Na, ⁵²Cr, ⁵⁵Mn, ⁵⁹Co, ⁶⁶Zn, ⁸⁵Rb, ⁸⁷Rb, ⁸⁹Y, ¹²⁷I, ¹³³Cs, and ¹⁹⁷Au, which produce radionuclides with half-life of more than 1 week by (γ , n) reaction. About 100 mg of high purity powder reagent (metal, oxide, or chloride) is wrapped in aluminum foil to be formed a disk (8 mm ϕ) except for Au. For Au, about 12 mg of a foil (8 mm ϕ) was used. The disks were placed in a quartz tube together with Ni monitor foils. Irradiations were performed for 60 min with bremsstrahlung beam of maximum end-point energy (E_0) of 30 MeV from KURRI-LINAC.

After irradiation, a target disk was taken out from a quartz tube and was put into a polyethylene bag. Gamma-spectrometry by a Ge detector was performed at radioisotope research facility, Tokyo Metropolitan University, after appropriate cooling. To reduce true coincidence effect a sample was placed at 30 cm far from a detector.

RESULTS: Relative reaction yields normalized with one of ⁵⁸Ni(γ , n)⁵⁷Ni reaction were obtained. Observed relative yields (γ , n) reaction at $E_0 = 30$ MeV are shown by closed circles in Fig.1 and relative yields of (γ , 2n) reactions for ⁵⁸Ni and ⁸⁵Rb are also shown by open circles. Open triangles present relative yield values of ⁵⁸Ni(γ , n)⁵⁷Ni reaction by using Ni powder and the values were 1.00 ± 0.06 and 1.01 ± 0.06 . These yields confirm that correct yield values were obtained by using different type of target and monitor, that is, a powdered target and a Ni foil monitor in this study.

As shown in Fig.1, relative yields of (γ , n) increase smoothly with increasing target mass. However, yield of ⁵⁸Ni(γ , n) is found to be not consistent with the trend and the yield value is about 3 times smaller than the trend. The trend observed in this study can help an estimation of (γ , n) reaction yields for various elements.

Yields of (γ , n) reaction producing a radionuclide with half-life of less than 1 week and at $E_0 = 20$ MeV will be determined in next year.

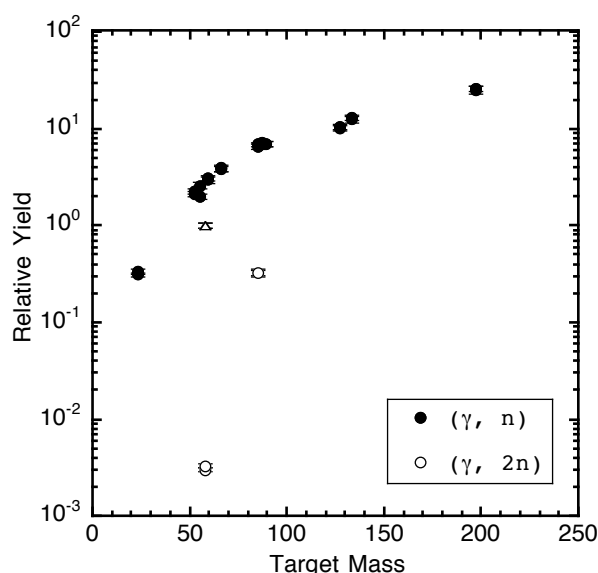


Fig. 1. Target mass yield for (γ , n) and (γ , 2n) reactions at $E_0 = 30$ MeV. Yield values normalized with a yield of ⁵⁸Ni(γ , n)⁵⁷Ni are shown.

CO2-2 Precise Measurements for Epi-Thermal Neutrons Using Two Different Scintillators

T. Matsumoto, H. Harano, A. Masuda, T. Kobayashi, Y. Yamamoto, H. Tomita, J. Kawarabayashi, T. Iguchi, A. Uritani, K. Watanabe, J. Hori, Y. Sakurai

National Metrology Institute of Japan, National Institute of Advanced Industrial Science and Technology

¹School of Engineering, Nagoya University

²Research Reactor Institute, Kyoto University

INTRODUCTION: Evaluation of neutron dose equivalent for the epi-thermal neutron region is very important in work places with neutron sources or nuclear fuels as well as irradiation fields in a boron neutron capture therapy. A new calibration method for the response of neutron dosimeters has been developed using a pulse white neutron beam[1]. On the other hand, it is not easy to measure precisely the neutron fluence for epi-thermal neutrons in an irradiation field, although a gold activation method is usually used in a thermal neutron region, and an elastic neutron scattering reaction with hydrogen atoms is adopted in a fast neutron region to measure precise neutron fluence. In the present study, we have developed a measurement method for epi-thermal neutrons using a ${}^6\text{Li}_6^{\text{nat}}\text{Gd}^{10}\text{B}_3\text{O}_9\text{:Ce+}$ (LGB) and an NaI(Tl) scintillators. We also developed an epithermal neutron camera consisting of GEMs and resonance filters for neutrons up to 10 keV.

EXPERIMENTS: A typical experimental setup is shown in Fig. 1. A neutron beam through collimators was obtained by the photoneutron reaction using a water-cooled tantalum target at the KURRI Linac [2]. The 50 mm-diameter and 5-mm thick LGB scintillator was set at the center of the neutron beam. The 76.2 mm-diameter and 76.2 mm thick NaI(Tl) was set out of neutron beam. When the LGB scintillator detects neutrons by the ${}^{10}\text{B}(n,\alpha\gamma)$ reaction, 478 keV monoenergetic gamma rays are produced and subsequently detected with the NaI(Tl) scintillator. In the coincidence measurements, the neutron capture reaction rate in the LGB scintillator is obtained without detection efficiencies of the LGB and the NaI(Tl) scintillators. Moreover, the absolute neutron fluence is determined by measuring gamma rays from the ${}^{10}\text{B}(n,\alpha\gamma)$ reaction with the NaI(Tl) scintillator in setting a thick ${}^{10}\text{B}$ total absorption sample in front of the LGB scintillator. The detection system were experimentally tested using the neutron beam from a neutron source with the photoneutron reaction by means of the TOF method. Fig.2 shows the pulse height spectra of the LGB scintillator with and without the coincidence measurements. In the LGB scintillator, neutrons are detected by the ${}^{10}\text{B}(n,\alpha\gamma)$ reaction as well as the ${}^6\text{Li}(n,\alpha)\text{T}$ reaction and the $\text{Gd}(n,\gamma)$ reaction. In Fig. 2, a

peak around 150 channel is caused by the ${}^{10}\text{B}(n,\alpha\gamma)$ reaction. The counts due to the ${}^6\text{Li}(n,\alpha)\text{T}$ reaction and the $\text{Gd}(n,\gamma)$ reaction are successfully rejected by the coincidence measurements.

Characteristics of a prototype of epithermal neutron imaging camera were also measured using the TOF method. The prototype detector consists of a silver plate as a resonance filter, a B_4C thermal neutron absorber, and a GEM with a neutron converter of ${}^{10}\text{B}$. The difference in observed counts from each readout electrode of GEMs between the measurements with and without the resonance filter gives the epithermal neutron image.

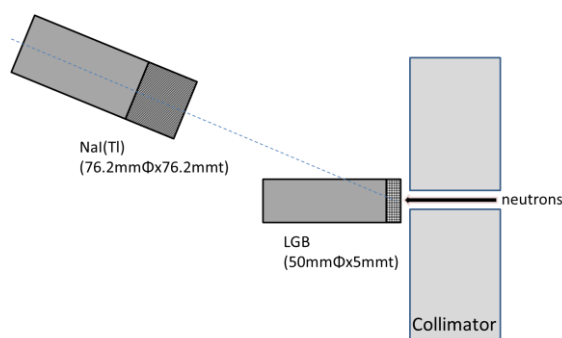


Fig. 1 Typical experimental setup

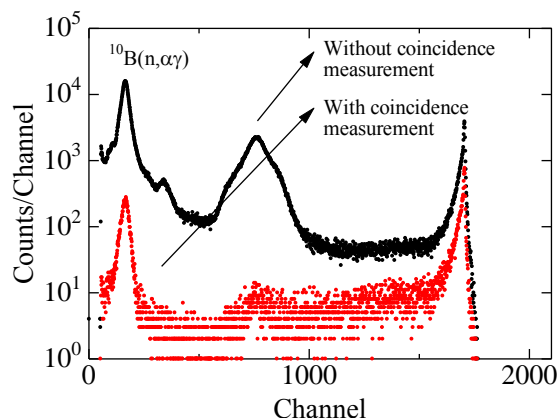


Fig.2 Pulse height spectra of the LGB scintillator with and without the coincidence measurements with the NaI(Tl) scintillator.

REFERENCES:

- [1] T. Masumoto *et al.*, KEK proc. 2011 (8), 218-225 (2012).
- [2] K. Kobayashi *et al.*, Annu. Rep. Res. Reactor inst. Kyoto Univ. 22, 142 (1989).

H. Yashima, J. Hori, Y. Takahashi and S. Nakamura¹

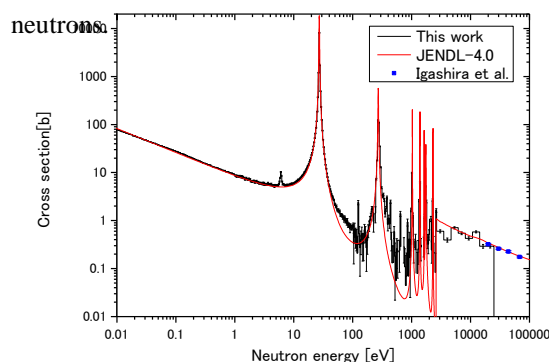
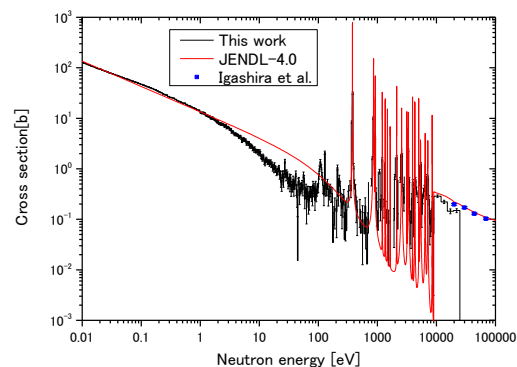
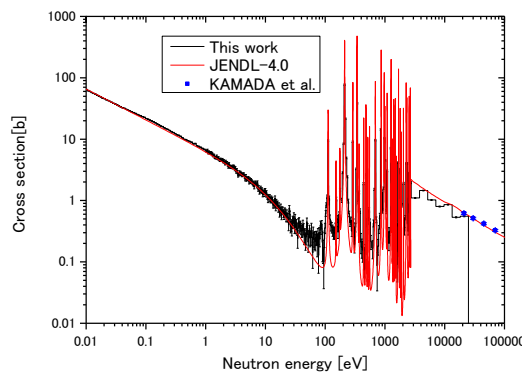
Research Reactor Institute, Kyoto University
¹Nuclear Science and Engineering Directorate, Japan Atomic Energy Agency

INTRODUCTION: Selenium-79 is one of the most important long-lived fission products in the transmutation study. However, there is no experimental data of neutron-capture cross sections for ^{79}Se because it is difficult to prepare its sample. Therefore, we have started a systematic measurement of neutron capture cross sections and gamma-ray spectra of stable Se isotopes in order to improve the evaluated neutron capture cross sections of ^{79}Se . In this work, we measured the neutron capture cross sections for ^{74}Se , ^{76}Se and ^{77}Se in the neutron energy range from 0.01 eV to 10 keV.

EXPERIMENTS: The measurements have been performed by the neutron time-of-flight (TOF) method using the 46-MeV electron linear accelerator at the Research Reactor Institute, Kyoto University (KURRI-LINAC). The neutron capture gamma-rays emitted from sample were detected by a total absorption spectrometer consisting of twelve $\text{Bi}_4\text{Ge}_3\text{O}_{12}$ (BGO) scintillators, which was placed at a distance of 12.7 m from the photo-neutron source of the KURRI-LINAC. Since base line fluctuations of signals from the BGO spectrometer were caused by the strong bremsstrahlung (gamma flush) synchronized with the accelerator pulse, a data taking system based on digital signal processing (DSP) technique was employed to correct them. A data set of TOF and pulse height (PH) was obtained by analyzing of waveform of the signals. Relative cross sections for ^{74}Se , ^{76}Se and ^{77}Se were obtained from the TOF spectra discriminated by the PH spectra and the incident neutron flux on the capture sample determined by the $^{10}\text{B}(n, \alpha\gamma)$ standard cross section, and then normalized by the evaluated value of capture cross section at the thermal neutron energy in JENDL-4.0[1].

RESULTS: Figures 1 to 3 show the neutron capture cross sections for ^{74}Se , ^{76}Se and ^{77}Se with previous experimental data and evaluated data[2, 3] in JENDL-4.0, respectively.

In Fig. 1, present results agree with previous results for keV neutrons and new resonances of ^{74}Se were found at 6, 123 eV. In Fig. 2, present results are smaller than previous results by about 10% for keV neutrons and there are large difference between present results and the values of JENDL-4.0. In Fig. 3, present results are smaller than previous results by about 10% for keV

Fig. 1 Neutron capture cross section for ^{74}Se .Fig. 2 Neutron capture cross section for ^{76}Se .Fig. 3 Neutron capture cross section for ^{77}Se .

This work is supported by JSPS KAKENHI (22226016).

REFERENCES:

- [1] K. Shibata *et al.*, JENDL-4.0: A New Library for Nuclear Science and Engineering, *J. Nucl. Sci. Technol.* **48**(1) (2011) 1-30.
- [2] M. Igashira *et al.*, Systematic study on keV-neutron capture reaction of Se isotopes, *J. Korean Phys. Soc.*, **59**(2) (2011) 1665-1669.
- [3] S. Kamada *et al.*, Measurements of keV-neutron capture cross sections and capture gamma-ray spectra of ^{77}Se , *J. Nucl. Sci. Technol.* **47**(7) (2010) 634-641

CO2-4 Measurement of Gamma Ray and Neutron Spectrum of Curium Isotope

Y. Nauchi, J. Hori¹ and T. Sano¹
 Central Research Institute of Electric Power Industry
¹Research Reactor Institute, Kyoto University

INTRODUCTION:

The yield ratio of higher energy (>3.5MeV) gamma ray to neutron in a spent fuel pond, (G/N), is linearly related to the sub-critical multiplication factor k_{sub} [1]. In the pond, (G/N) for $k_{sub}=0$ is determined by the radioactive decay of Curium (Cm) isotopes. In order to estimate k_{sub} by a measurement of (G/N), spectra and intensities of the radiations from the Cm isotopes are essential. However, no data are reported for the gamma ray and only a few data are done for the neutron [2]. For the reason, measurements of them are launched in KUR-LINAC.

NEUTRON MEASUREMENTS:

The Cm sample was electrodeposited on stainless steel disk (0.17mm in thickness) and enclosed in a cylindrical fission chamber made of aluminum. The mass ratio of isotopes, $^{244}\text{Cm} / ^{246}\text{Cm} / ^{248}\text{Cm} = 0.00057 / 11.1 / 258$. Its neutron source intensity was expected $1.07 \times 10^4 \text{s}^{-1}$. Neutrons from the sample were measured with an NE213 scintillator of 5.08cm in thickness and 5.08cm in diameter, which is set at 5.2cm from the sample. Pulse heights of the neutrons are calibrated in the electron light unit with $^{241}\text{Am-Be}$ and ^{60}Co gamma ray sources. Neutron events counted in the detector were identified by the pulse shape discrimination (PSD) technique. Neutrons from a ^{252}Cf source were also measured. The measured pulse height spectrum for the Cm sample (No-coin.) is found very similar to that of ^{252}Cf as shown in Fig 1. We also performed coincidence measurements of a fission fragment and a neutron. In the case (coin), count rate of lower energy neutron decreases as shown in Fig. 1. In the lower energy region, PSD spectra of neutron and gamma ray are slightly overlapped so some gamma ray events are included in the neutron pulse height spectrum. The decrement of the count rate by the coincidence might be due to discrimination of lower energy gamma rays from short lived nuclides generated by neutron absorptions. To clarify the decrement, a time of flight measurement of neutron is required.

GAMMA RAY MEASUREMENTS:

In order to measure higher energy gamma rays with higher efficiency and higher resolution, a BGO scintillator of 7.62cm in diameter and 7.62cm thick and HP-Ge detector of the 20% relative efficiency were employed. To reduce direct interactions of neutron in the scintillator, polyethylene blocks of 25cm thickness was set between the Cm sample and detectors as shown in Fig. 2. The gamma ray pulse height spectra in the detectors for the Cm sample are also similar to those of ^{252}Cf as shown in Fig.3. In addition to the 2.2MeV peak of H(n, γ) reaction, continuum spectra from 3 to 5.5MeV are observed for the

Cm sample and ^{252}Cf . In the BGO spectra, some bump structures are found in 6-10MeV region. They might be attributed to some neutron induced reactions such as $^{56}\text{Fe}(n,\gamma)$ in the iron plate or $^{73}\text{Ge}(n,\gamma)$ in detectors, although peak spectrum is not identified in the HP-Ge. We shall perform another experiment to identify whether such bumps are caused by gamma rays directly from the spontaneous fission of the Cm samples or not.

REFERENCES:

- [1] Y. Nauchi *et al.*, Proc. PHYSOR2012, Oct. 7-10, 2002, Seoul, 1C-03 on CD-ROM.
 [2] EXFOR: Experimental Nuclear Reaction Data, <http://www.oecd-nea.org/dbdata/x4/> on Internet.

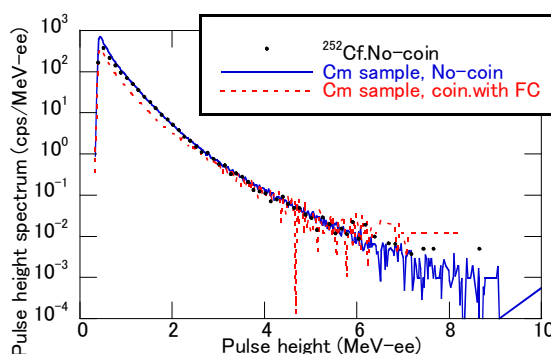


Fig.1 Neutron pulse height spectrum in NE213 for Cm sample and ^{252}Cf . Coincidence / No-Coincidence cases with fission chamber signal.

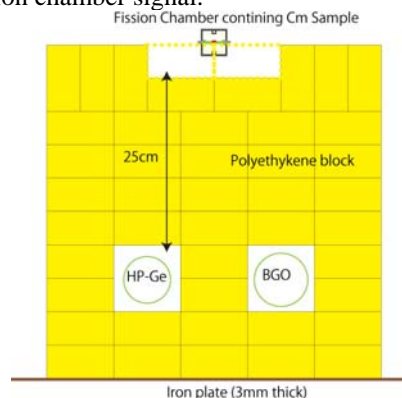


Fig. 2. Schematic view of gamma ray measurement.

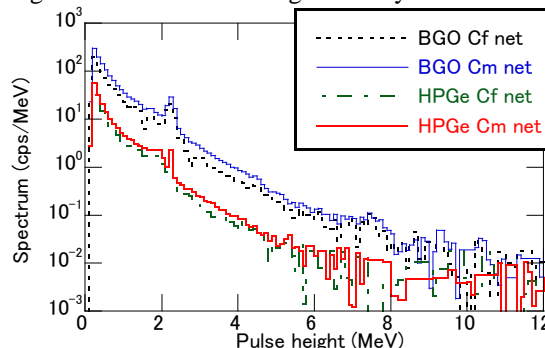


Fig. 3 Gamma ray pulse height spectrum in BGO scintillator for Cm sample and ^{252}Cf .

CO2-5 Measurements of Thorium-Fueled Core Characteristics and Replacement Worth of Thorium Plates to Aluminum Plates (3)

T. Kitada, T. Fujii, K. Wada, Vu Thanh Mai, N. Takaki¹, T. Katou¹ and H. Unesaki²

Graduate School of Engineering, Osaka University
¹Cooperative Major in Nuclear Energy, Tokyo City University
²Kyoto University Research Reactor Institute

INTRODUCTION: Thorium is widely known as a good candidate of Uranium, and is considered as a next generation fuel. However the accuracy of the cross section is quietly lower than that of Uranium because the number of experiments with Thorium is not so many and also validation study is not enough.

The object of this experiment series is to validate the Thorium cross section through the comparison between calculation and measured results for Thorium-fueled core characteristics and replacement worth of Thorium plates to Aluminum plates at various spectrum fields with different unit fuel cell.

EXPERIMENTS: The assembled core is the first core to be critical with the unit fuel cell named “10/8PETEETEE-r1” which is shown in Fig. 1. This unit fuel cell is the same composition to the fuel cell named “10/8PETEETEE”, but the difference is in the order of each plates.

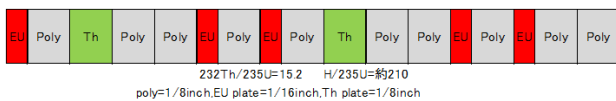


Fig.1 Unit Fuel Cell (10/8)PETEETEE-r1)

In the experiment, critical approach was performed. The number of fuel assembly and control rod arrangements at critical were analyzed before the experiment so as to match the constraints (maximum excess reactivity and control rod worth). The core arrangements at each step are illustrated in Fig. 2.

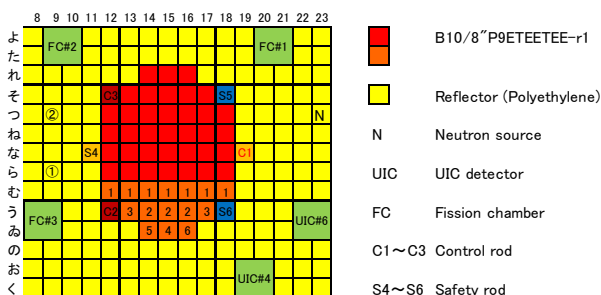


Fig. 2 Core arrangements at each step from initial core to critical core (B10/8)P9ETEETEE-r1)

The number marked in fuel assemblies in Fig.2 shows the fuel assemblies added at each step of critical approach.

Initial core were assembled by 36 fuel assemblies, and at next step fuel assemblies marked as “1” in Fig. 2 were added to measure count rate by fission chambers and BF₃ detector marked as “①” and “②”. The number of fuel assemblies was gradually increased, and the critical core were realized at last step:6 with 51 fuel assemblies. The inverse count rate ratio curve obtained through the critical approach is shown in Fig. 3 for the case of all control rods withdrawn(j=3).

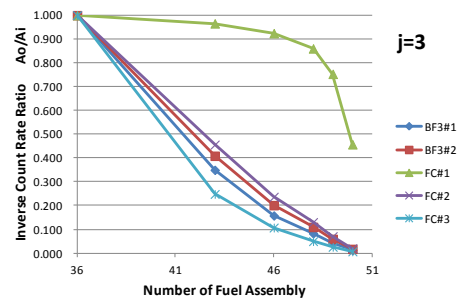


Fig.3 Inverse count rate ratio curve obtained for B10/8)P9ETEETEE-r1 core

The excess reactivity was measured by the period method and the value is about 0.23 [%dk/k], and the control rod worth for C1, C2 and C3 measured by rod drop method are 0.260, 0.270 and 0.269 [%dk/k], respectively. These values satisfy their constraints to operate the core.

The core shown in Fig.2 was slightly changed to low excess reactivity state so as to measure the replacement worth. Thorium plates were replaced to Aluminum plates to measure the replacement worth by the change in excess reactivity. The position of the replacement was the center fuel assembly named 15 and the number of the replacement was two or four at around the center in core height. This measurement was done to check the C1 rod position at critical with different replacement situation, because the calibration curve of C1 rod obtained by fitting many experimental results (period method) was confirmed to have enough accuracy to check the excess reactivity. The results are summarized in Table 1, and the results are roughly good agreement in the analysis with continuous energy Monte-Carlo code with JENDL-4.0.

Table 1 Measured results of excess reactivity

	excess [Δ k/k]	error [Δ k/k]
partial	7.83E-04	3.38E-06
partial + Al (2)	2.11E-03	5.83E-06
partial + Al (4)	3.34E-03	6.96E-06

RESULTS: Thorium-fueled core which has never assembled at KUCA was assembled. Criticality approach and related measurements were successfully performed. The detailed analysis of the results is in progress.

Measurements of Replacement Worth of Thorium Plates to Aluminum Plates at EE1 Core

T. Kitada, T. Fujii, K. Wada, Vu Thanh Mai, T. Kojima, T. Mishiro, N. Takaki¹, T. Katou¹ and H. Unesaki²

Graduate School of Engineering, Osaka University
¹Cooperative Major in Nuclear Energy, Tokyo City University
²Kyoto University Research Reactor Institute

INTRODUCTION: Thorium is widely known as a good candidate of Uranium, and is considered as a next generation fuel. However the accuracy of the cross section is quietly lower than that of Uranium because the number of experiments with Thorium is not so many and also validation study is not enough.

The object of this experiment is to validate the Thorium cross section through the comparison between calculation and measured results for replacement worth of Thorium plates to Aluminum plates at various spectrum fields with different unit fuel cell.

EXPERIMENTS: The assembled core named EE1 core is the core that the characteristics are already measured. The core arrangement to measure the replacement worth of Thorium plates is shown in Figure 1.

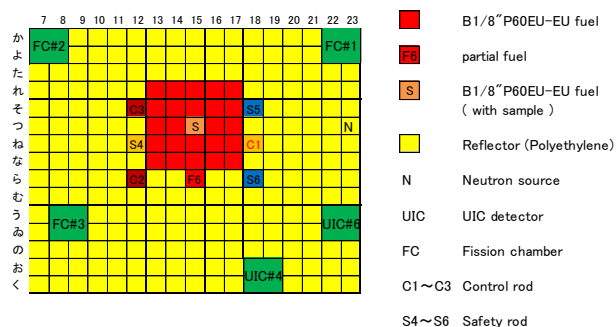


Fig. 1. Core arrangement (B1/8''P60EU-EU(5))

The excess reactivity was measured by the period method and adjusted so as to measure the replacement worth easily by using partial fuel (6 fuel cells) at β 15. It should be mentioned that the excess reactivity was increasing during the experiment, therefore the number of the fuel cell at partial fuel was decreased from 6 to 4 at the later stage of the experiment to satisfy the constraints of KU-CA operation.

The fuels are assembled as shown in Figure 2.

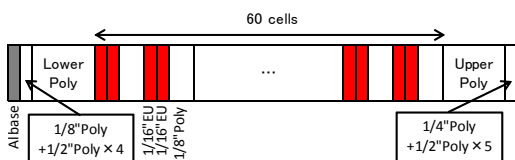


Figure 2 (a) Fuel assembly (1/8''P60EU-EU)

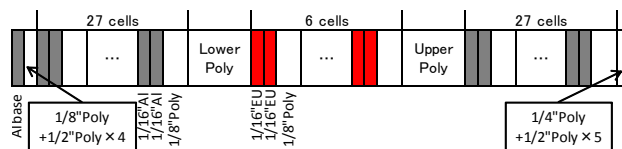


Figure 2 (b) Partial fuel assembly (6 fuel cells)

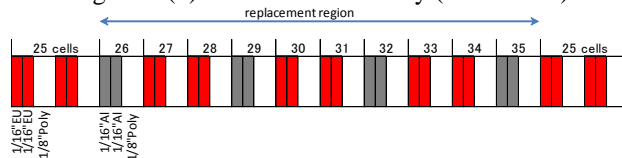


Figure 2(c) Fuel cell arrangement for replacement worth measurement (Al plates are replaced by Thorium plates)

As shown in Fig.2(c), the replacement positions are around the central in core height and not adjacent so as to reduce the interference effect in neutron flux caused by Thorium plates. The excess reactivity with/without Thorium plates were measured by checking the C1 rod position after confirming the accuracy of C1 rod curve by fitting many experimental results obtained by the period method. The obtained fitting curve is shown in Figure 3.

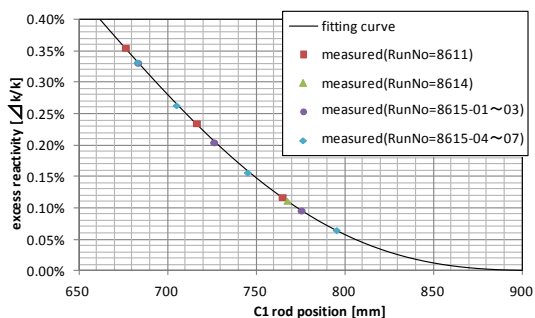


Fig. 3. C1 rod curve used for replacement worth measurements

The measured results are summarized in Table 1, and the results are roughly good agreement in the analysis with continuous energy Monte-Carlo code with JENDL-4.0.

Table 1. Measured results of excess reactivity

	excess $[\Delta k/k]$	error $[\Delta k/k]$
partial_1 + Al (4)	3.38E-03	2.9E-06
partial_1 + Th (4)	1.16E-03	3.7E-06
partial_2 + Al (4)	2.84E-03	1.6E-06
partial_2 + Th (4)	5.99E-04	2.0E-06

partial_1 : 6 fuel cells, partial_2 : 4 fuel cells in the partial fuel

RESULTS: The replacement worth of Thorium plates to Al plates were successfully measured at B1/8''P60EU-EU core where the neutron spectrum is hard compared to the former core arrangement(CA2405). The detailed analysis of the results is in progress.